

Seasonal Variability of Ice Motion for Hubbard and Valerie Glaciers, Alaska

Courtney Bayer,^{1,2,3} Wesley Van Wychen,¹ Anna Wendleider⁴ and Brittany Main^{1,5}

(Received 8 March 2024; accepted in revised form 10 September 2024)

ABSTRACT. Hubbard Glacier is a large, fast-flowing, tidewater-terminating glacier in the Saint Elias Mountains. It is connected at its terminus to Valerie Glacier. Although Hubbard Glacier has been shown to experience large intra-annual velocity changes and a long-term deceleration, previous seasonality studies have had limited timescales without a dense record of motion. Valerie Glacier's variability has also been understudied, with only one study reporting its seasonal behaviour. The goal of the current study was to combine ITS_LIVE, RADARSAT-2, RADARSAT Constellation Mission, and TerraSAR-X/TanDEM-X-derived velocity data to create the densest record of motion ever constructed for Hubbard and Valerie glaciers for a period from July 2013 to April 2022, in order to explore seasonal velocity variability of both glaciers. We used air temperature (NCEP-NCAR Reanalysis) to estimate surface melt on the glaciers, which we explored as a potential driver for seasonal velocity changes. Valerie Glacier had a seasonal pattern of fast flow in May, with minimum flow between August and November before accelerating again. We found a unique seasonal pattern that has not been previously observed on Hubbard Glacier, with two periods of fast motion: one in May and one in December–February. Considering our findings and insights from other recent research, we inferred that the spring peaks and late summer/fall minimums on both glaciers are due to meltwater reaching the glacier bed and influencing the subglacial hydrology. We did not determine the cause of the winter peak and slight velocity drop before the spring peak on Hubbard Glacier, suggesting this should be a topic for future studies, although we hypothesize that the glacier's geometry influences these changes.

Keywords: glaciers; ice dynamics; remote sensing; synthetic aperture radar (SAR); seasonality; climate change; melt; subglacial hydrology

RÉSUMÉ. Le glacier Hubbard est un vaste glacier à écoulement rapide qui se termine à l'eau de marée, dans la chaîne Saint-Élie. Il rejoint le glacier Valerie. Même si le glacier Hubbard présente d'importantes variations intra-annuelles en termes de vitesse et une décélération à long terme, il y a eu peu d'études de saisonnalité antérieures sans enregistrement de mouvement dense. De plus, la variabilité du glacier Valerie n'a pas été suffisamment étudiée, une seule étude se concentrant sur son comportement saisonnier. La présente étude visait à fusionner les données de vitesse obtenues à partir d'ITS_LIVE, de RADARSAT-2, de la mission de constellation RADARSAT et de TerraSAR-X/TanDEM-X pour créer l'enregistrement de mouvement le plus dense jamais réalisé pour les glaciers Hubbard et Valerie, couvrant la période allant de juillet 2013 à avril 2022. Cet enregistrement avait pour but d'analyser la variation saisonnière de la vitesse de ces deux glaciers. Nous avons utilisé la température de l'air (réanalyse NCEP-NCAR) pour estimer la fonte de surface des glaciers, que nous avons considérée comme un possible facteur de déclenchement des variations saisonnières de vitesse. Le glacier Valerie avait un régime saisonnier d'écoulement rapide en mai, avec un débit minimal d'août à novembre, avant de s'accélérer à nouveau. Nous avons remarqué un régime saisonnier unique jamais observé sur le glacier Hubbard, caractérisé par deux périodes de mouvement rapide : une en mai et une autre de décembre à février. À la lumière de nos constatations ainsi que des informations issues d'autres études récentes, nous en concluons que les périodes de pointe du printemps et les minima de la période de la fin de l'été et de l'automne pour les deux glaciers s'expliquent par le fait que l'eau de fonte atteint le lit glaciaire, influençant ainsi l'hydrologie sous-glaciaire. Nous n'avons pas déterminé la raison de la période de pointe hivernale et de la faible baisse de vitesse observée juste avant la période de pointe du printemps sur le glacier Hubbard. Ce sujet pourrait faire l'objet d'autres études. Toutefois, nous proposons comme hypothèse que la géométrie du glacier joue un rôle dans ces changements.

Mots-clés : glaciers; dynamique des glaces; télédétection; radar à synthèse d'ouverture (SAR); saisonnalité; changement climatique; fonte; hydrologie sous-glaciaire

Traduit pour la revue *Arctic* par Nicole Giguère.

¹ Department of Geography and Environmental Management, University of Waterloo, 200 University Avenue West, Waterloo, Ontario N2L 3G1, Canada

² Current address: Meteorological Research Division, Environment and Climate Change Canada, 2121 Transcanada Route, Dorval, Québec H9P 1J3, Canada

³ Corresponding author: cabayer@uwaterloo.ca

⁴ German Aerospace Centre, Oberpfaffenhofen, Münchner Straße 20, 82234 Weßling, Germany

⁵ Department of Geography, Environment and Geomatics, University of Ottawa, Simard Hall, 60 University Private, Ottawa, Ontario K1N 6N5, Canada

INTRODUCTION

Hubbard Glacier, which originates on Mount Logan's flank at 5959 m (Yukon, Canada) and shares névés and divides with other valley glaciers (such as Kaskawulsh and Logan glaciers), flows >120 km to sea level, where it terminates in Disenchantment Bay and Russell Fjord (Yakutat Bay, Alaska) (Fig. 1; Clarke and Holdsworth, 2002; Ritchie et al., 2008; Stearns et al., 2015). It is significant globally as the largest tidewater glacier outside of the poles, with a grounded calving front previously measured to be 11.4 km wide (Meier and Post, 1987; Trabant et al., 2003; Ritchie et al., 2008). Valerie Glacier is a smaller adjacent tributary glacier of Hubbard Glacier contributing ice into the western edge of Hubbard Glacier's terminus, with a medial moraine between the two glaciers marking their separation (Fig. 1; Mayo, 1988; Ritchie et al., 2008).

Understanding glacier dynamics and how they are evolving for Hubbard and Valerie glaciers is important because it can assist with the improvement of mass balance projections for mountain glaciers. Currently, these projections are limited by inadequate understanding and low temporal resolution of tidewater glacier dynamics (Burgess et al., 2013a). Improving the models can ultimately improve our current understanding of the glaciers' impact on sea level rise. Hubbard Glacier is known for its high velocities and is one of 12 fast-flowing glacial systems in Alaska identified by Burgess et al. (2013a) with velocities higher than 1 m/d over much of its length due to its linkage to high accumulation rates (Burgess et al., 2013a; Waechter et al., 2015; Van Wyk et al., 2018). Although long-term velocity trends on Hubbard Glacier have been difficult to determine because of sparse measurements and large seasonal variation in flow speeds (Stearns et al., 2015), when the variable of seasonal variability was removed, this glacier was found to have decelerated from 7.7 m/d in 1978 to 6.0 m/d in 1997 (Trabant et al., 2003). Broadly, glacier dynamics in Alaska are known to vary interannually, and winter velocities have shown synchronicity throughout the region, which suggests that Alaskan glaciers likely have a common hydrological mechanism driving velocity changes (Burgess et al., 2013b). In support of this idea, Yang et al. (2022) found that different glacier types within the Kenai Peninsula in Alaska showed similar seasonal flow patterns, which they suggested was due to regional-scale meteorological processes.

In terms of interannual velocity changes, Stearns et al. (2015) found that Hubbard Glacier experienced significant variability in flow speeds, ranging from ~4.1 to ~14 m/d, with the faster flow occurring over most regions of Hubbard Glacier's terminus in April/May and the slowest flow in October/November. Similarly, Trabant et al. (2003) determined large seasonal variability in Hubbard Glacier's terminal lobe of up to ~2 m/d, with maximum flow speeds observed in May and June and minimum flow speeds in September and November. These general patterns of variability in ice motion follow the usual seasonality in

Alaskan tidewater and land-terminating glaciers (Stearns et al., 2015; Armstrong et al., 2017). However, despite the work of Stearns et al. (2015), Trabant et al. (2003), and the known large variability of flow speeds observed on Hubbard Glacier, the characterization of the seasonality of glacier motion for Hubbard glacier remains largely unresolved.

Regarding Valerie Glacier, much of the previous research has been related to pulsing activity (in 1986, August 1993–August 1995, and July 2000–September 2002), where velocities reached higher than ~36 m/d in 1986 (Mayo, 1988, 1989; Ritchie et al., 2008). Few studies have investigated the seasonal flow patterns of Valerie Glacier, although Trabant et al. (1991) analyzed its velocity from ~1986–1989, finding large seasonal variations (flow speeds near the confluence to Hubbard Glacier in this period ranged from ~2.74 m/d to ~5.48 m/d). Stearns et al. (2015) investigated seasonality at different sections along Hubbard Glacier's terminus and found that the region with ice flowing in from Valerie Glacier had a slightly different pattern than other regions of Hubbard Glacier's terminus, with the highest velocities in July–August. A long-term flow pattern of Valerie Glacier has not been reported in previous work.

Over the past few decades, remote sensing data has become increasingly available with the launch of new sensors, for example, RADARSAT-2 and TerraSAR-X launched in 2007 (Airbus Defence and Space, 2014; Government of Canada, 2021), TanDEM-X in 2010 (Airbus Defence and Space, 2014), Sentinel-1A in 2014, Sentinel-1B in 2016 (The European Space Agency, 2021), and RADARSAT Constellation Mission in 2019 (Government of Canada, 2021). With more remote sensing data available, velocity trends of Hubbard and Valerie glaciers can now be determined in a higher temporal resolution than has been analyzed in the past. Given this background, the goals of this work are to utilize a large catalogue of remote sensing data in order to: (1) build a dense record of ice motion for Hubbard and Valerie glaciers that can be used to resolve the seasonality of both glaciers over the last decade, and (2) use records of climate data to explore the seasonal drivers of ice dynamics at Hubbard and Valerie glaciers.

METHODS

Velocity Data

GAMMA Remote Sensing Data: Velocity measurements over Hubbard and Valerie glaciers were generated from intensity offset tracking of Synthetic Aperture RADAR (SAR) data (TerraSAR-X/TanDEM-X [TSX/TDX], RADARSAT-2 [R2], and RADARSAT Constellation Mission datasets [RCM]) using GAMMA RS software. GAMMA software reads SAR single look complex (SLC) images and uses an intensity cross-correlation algorithm to determine the displacement between a reference and secondary image (Strozzi et

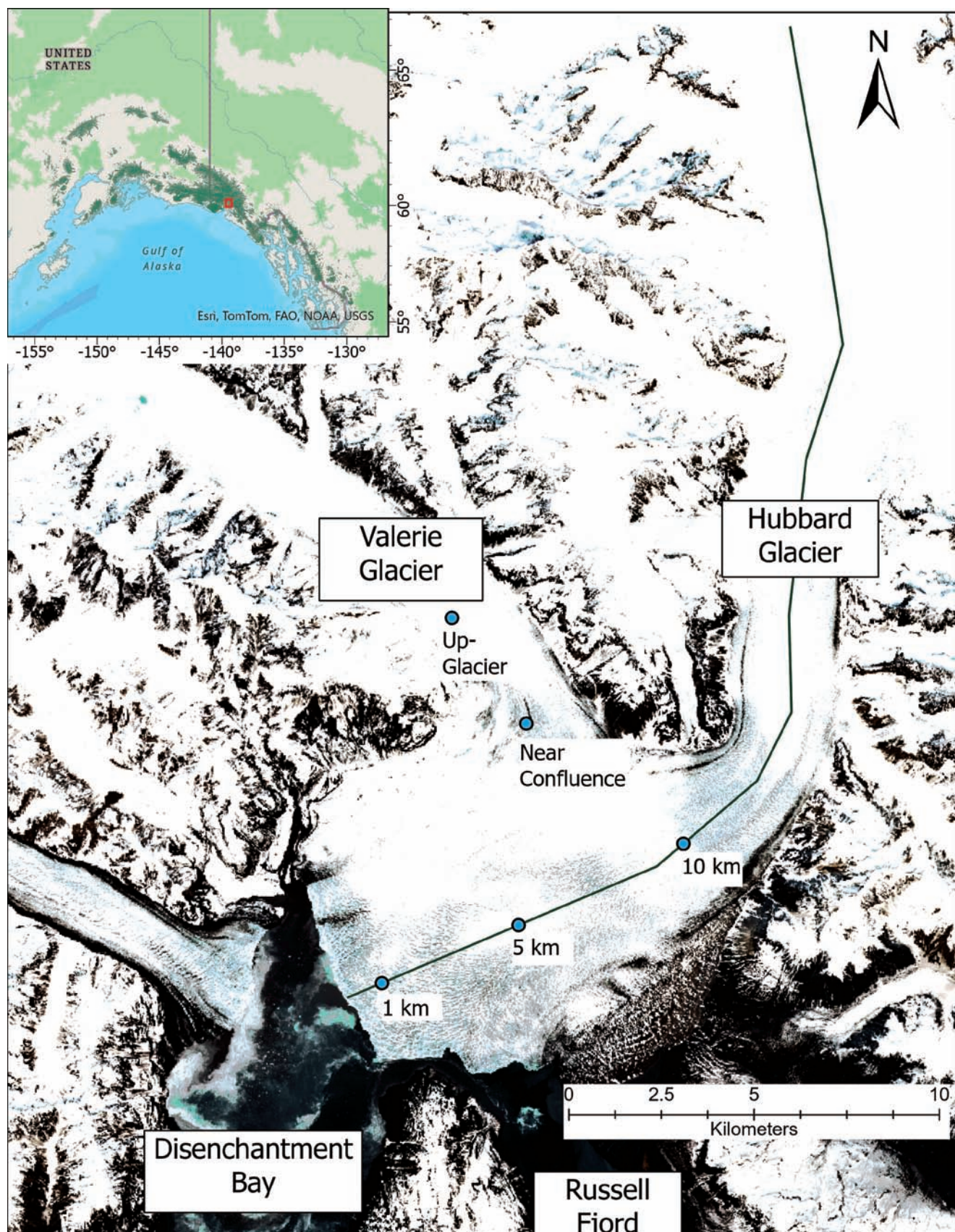


FIG 1. Hubbard Glacier and Valerie Glacier, showing Hubbard Glacier's centerline, with locations of data extraction marked at 1 km, 5 km, and 10 km from the terminus (in WGS 84 UTM Zone 7N). Two points on Valerie Glacier near the confluence of Hubbard Glacier and further up-glacier show the locations of data extraction. Inset: Alaskan glaciated regions (RGI Consortium, 2017) with red box showing the location of Hubbard Glacier (Esri World Topographic Map, in WGS 84 Web Mercator). Optical imagery: Sentinel-2 from 11 June 2021.

al., 2002). For further details on the creation of velocity products from GAMMA see Supplementary Appendix 1.

Once completed, the GAMMA workflow outputs the calculated displacements in a geocoded GeoTIFF file. Displacements of the GAMMA outputs are scaled to meters of displacement between the two images that are then transformed to the common unit of m/d. The uncertainty of glacier velocities from offset tracking is provided in Table 1.

ITS_LIVE Data: Pre-derived glacier velocity products for Hubbard and Valerie glaciers were retrieved from NASA MEaSUREs' Inter-Mission Time Series of Land Ice Velocity and Elevation (ITS_LIVE) widget (Gardner et al., 2022). This program provides global data on the surface velocity and elevation change of glaciers and ice sheets derived from Sentinel-1, Sentinel-2, and Landsat 7, 8, and 9 image datasets (Gardner et al., 2021). Image-pair velocities of Alaska and western North America were determined using the autonomous repeat image feature tracking (auto-RIFT) algorithm between repeated acquisitions, with Sentinel-2 and Landsat satellite imagery used if cloud cover was $\leq 60\%$ (Gardner et al., 2021). Gardner et al. (2018) provide full documentation on the methods used for this dataset and offer an uncertainty estimate of ~ 0.055 – 0.082 m/d. These products have a pixel resolution of 120 m and were constrained to a time separation between images of 7–30 days, which allowed us to obtain a sub-monthly temporal resolution of the dynamics of both Hubbard and Valerie glaciers between July 2013 and April 2022. Data is more scarce towards the beginning of the ITS_LIVE record, with the density of velocity products in the dataset increasing at the end of 2016 as a result of the launch of additional sensors (European Space Agency, 2020, 2021; Gardner et al., 2021; U.S. Geological Survey, 2022).

We downloaded Hubbard Glacier data at three points corresponding to 1 km (60.0137, -139.5069), 5 km (60.027, -139.4402), and 10 km (60.0458, -139.3594) from its terminus along its centerline (determined from manual selection while using optical imagery as a reference) to show how its velocity behaviour changed when moving up-glacier, away from the terminus. Valerie Glacier data was downloaded at two locations, the near confluence point (60.0758, -139.4337) and the up-glacier point (60.1018, -139.4687), to evaluate the velocity fluctuations near the confluence of Valerie Glacier and Hubbard Glacier and at a location further removed from the influence of Hubbard Glacier (points shown in Fig. 1).

Glacier Velocity Extraction: To provide a detailed determination of the seasonal variability of both Hubbard and Valerie glaciers, the velocity data from all sources (ITS_LIVE data and GAMMA RS data) were analyzed at five locations: three locations on Hubbard Glacier and two locations on Valerie Glacier (as described for the ITS_LIVE data), from July 2013 to April 2022. The combined velocity dataset resulted in 1296 velocity samples at Hubbard Glacier's 1 km location, 1407 velocity samples at Hubbard Glacier's 5 km location, and 923 velocity samples at Hubbard Glacier's 10 km location. For Valerie Glacier,

TABLE 1: Errors of TSX (Samo, 2022), RCM (Van Wychen et al., 2023), and R2 (Van Wychen et al., 2016) used in offset tracking.

SAR Sensor	Error
TSX	~ 0.016 m/d
RCM	~ 0.018 m/d
R2	~ 0.024 m/d

1273 velocity samples were obtained at the confluence location, and 994 velocity samples at the up-glacier point.

Melt Analysis

We analyzed climate using reanalysis data from NCEP-NCAR Reanalysis 1 (Kalnay et al., 1996) provided by NOAA PSL, Boulder, Colorado, USA (NOAA, 2025). We downloaded mean daily surface air temperatures (sigma level 995) for 2013–22 and used these to calculate the number of positive degree day (PDD) sums for each month. The reanalysis surface air temperature products are provided on a $2.5^\circ \times 2.5^\circ$ grid, and the grid cell located at 60, -140 was chosen to capture the climate at Hubbard Glacier (60.045, -139.39). To calculate monthly PDD sums, whenever the mean surface air temperature of individual days within the month was above 0° C, we cumulatively summed those values.

RESULTS

Spatial Velocity Structures

Figure 2 provides the general velocity structure of Hubbard and Valerie glaciers. With respect to Hubbard Glacier, higher velocities are found close to its terminus, where the glacier front meets the ocean. Moving up-glacier from the terminus, glacier velocities decrease to reach a minimum ~ 5.6 km from the terminus. After this point, velocities increase again and reach a maximum ~ 11.4 km from the terminus, where the glacier is constricted between valley walls and has a relatively steep slope. Although this spatial pattern of ice motion is observed at all times, glacier motion displayed great temporal variability. Valerie Glacier experiences faster velocities up-glacier, away from its terminus, although large seasonal variations in its velocity are also observed.

Seasonality

Figure 3a–e presents the velocity structure of Hubbard and Valerie glaciers for July 2013 to May 2022 from the extracted remote sensing-derived displacement maps at five distinct locations (identified with teal dots on Fig. 1). Seasonality of glacier motion is much more detailed after 2016 due to the wider availability of glacier velocity maps after this time, and 2022 data does not cover the full year. As such, the description and quantification of glacier

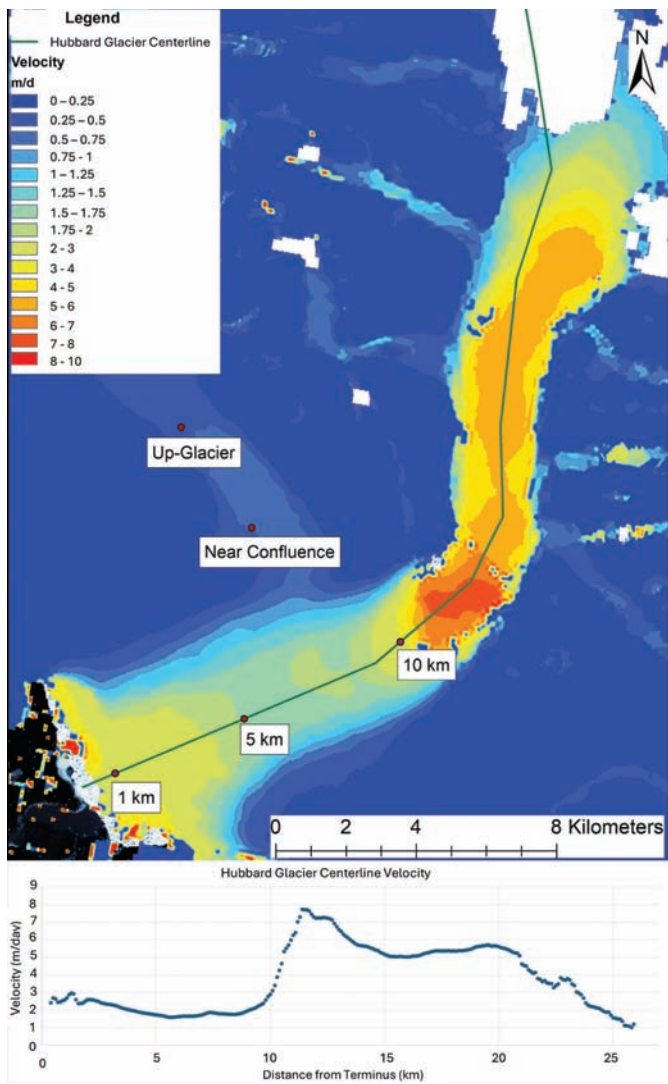


FIG 2. Glacier velocities of Hubbard and Valerie glaciers from TSX data on 21 August 2015 to 1 September 2015 (optical imagery: Sentinel-2 imagery from 11 June 2021, in WGS 84 UTM Zone 7N).

motion that follows focuses on the time period of January 2017 to January 2022.

Seasonally, two velocity peaks and two velocity drops were observed each year at all three locations on Hubbard Glacier (Fig. 3a–c). This velocity pattern was most evident at the location 1 km from the terminus, with the same pattern, albeit with a much smaller amplitude, also observed at the 5 km and 10 km points. Therefore, this discussion is focused on the 1 km point. At this location, one velocity peak occurred in the winter months (varying between December and February in different years) before velocities dropped slightly and reached a minimum between the end of January to April (again, varying between years). At 1 km from the terminus, maximum velocities during this winter peak occurred in January 2020, when Hubbard Glacier's velocity exceeded ~ 13 m/d. In this study period, the minimum values in the drop after this peak reached lower than ~ 5.0 m/d (as seen in March 2021). The relative decrease between this winter peak and following minimum

was generally less than ~ 5.2 m/d, although velocities decreased as much as ~ 7.9 m/d from January to April 2020. Velocities increased after this minimum to a second velocity peak in the spring (fastest velocities in May), where velocities at 1 km from the terminus reached higher than ~ 9.6 m/d at its maximum (May 2019). After this spring peak, velocities dramatically decreased, with this drop often greater than what occurred after the winter velocity peak, to reach minimum velocities in the late summer/fall (between August and October). These were the slowest velocities of the year, reaching as low as 0.77 m/d at 1 km from the terminus (September 2018). This relative decrease in velocity was always larger than ~ 5.5 m/d and decreased more than ~ 8.2 m/d in 2018. It was variable if the winter peak was higher than the following spring peak each year.

Unlike Hubbard Glacier, Valerie Glacier (Fig. 3 d, e) only experienced one seasonal velocity peak and velocity decrease each year. The velocity peak occurred in spring (generally in May) after a gradual acceleration from the winter until this peak. Velocities were observed to reach higher than ~ 4.4 m/d at the near confluence point and ~ 4.8 m/d at the up-glacier point. Following this peak, velocities decreased rapidly until dropping to Valerie Glacier's minimum velocities, then plateauing at this low flow speed in late the fall, with velocities as low as ~ 0.055 m/d at the near confluence point (September to November) and ~ 0.22 m/d at the up-glacier point (August–September). After the minimum velocities, flow speeds gradually increased until the spring peak was reached again. This pattern was consistent in all years analyzed.

Positive Degree Days and Climate Analysis

Figure 3f shows the PDD sums from 2013–22, with the analysis also focusing on January 2017 to December 2021 to allow for a direct comparison to seasonal velocity trends. The general PDD sum seasonal cycle is described in this discussion, although some years may have differences in the timing of increases and decreases of values. Generally, January to March had minimal PDD sums ($<10^{\circ}\text{C}$), with March–April PDD sums increasing but still small ($<25^{\circ}\text{C}$). The increasing PDDs coincided with increasing velocities on Valerie Glacier until its peak velocities around May. Similarly, Hubbard Glacier's velocities began to increase around April until the peak in May. After April, PDD sums continued to increase until reaching the maximum in July–August (maximum values in July 2019 reaching $\sim 370^{\circ}\text{C}$), with minimum velocities following close after these maximum PDD sum values (August to October for Hubbard Glacier, August to November for Valerie Glacier). After the maximum PDD sums, values began to decrease but were still relatively high until September–October ($>100^{\circ}\text{C}$). Following this and until the end of the year, values kept decreasing and became minimal again around November–December ($<6^{\circ}\text{C}$, although maximum December PDD sum of $\sim 17^{\circ}\text{C}$ occurred in 2017).

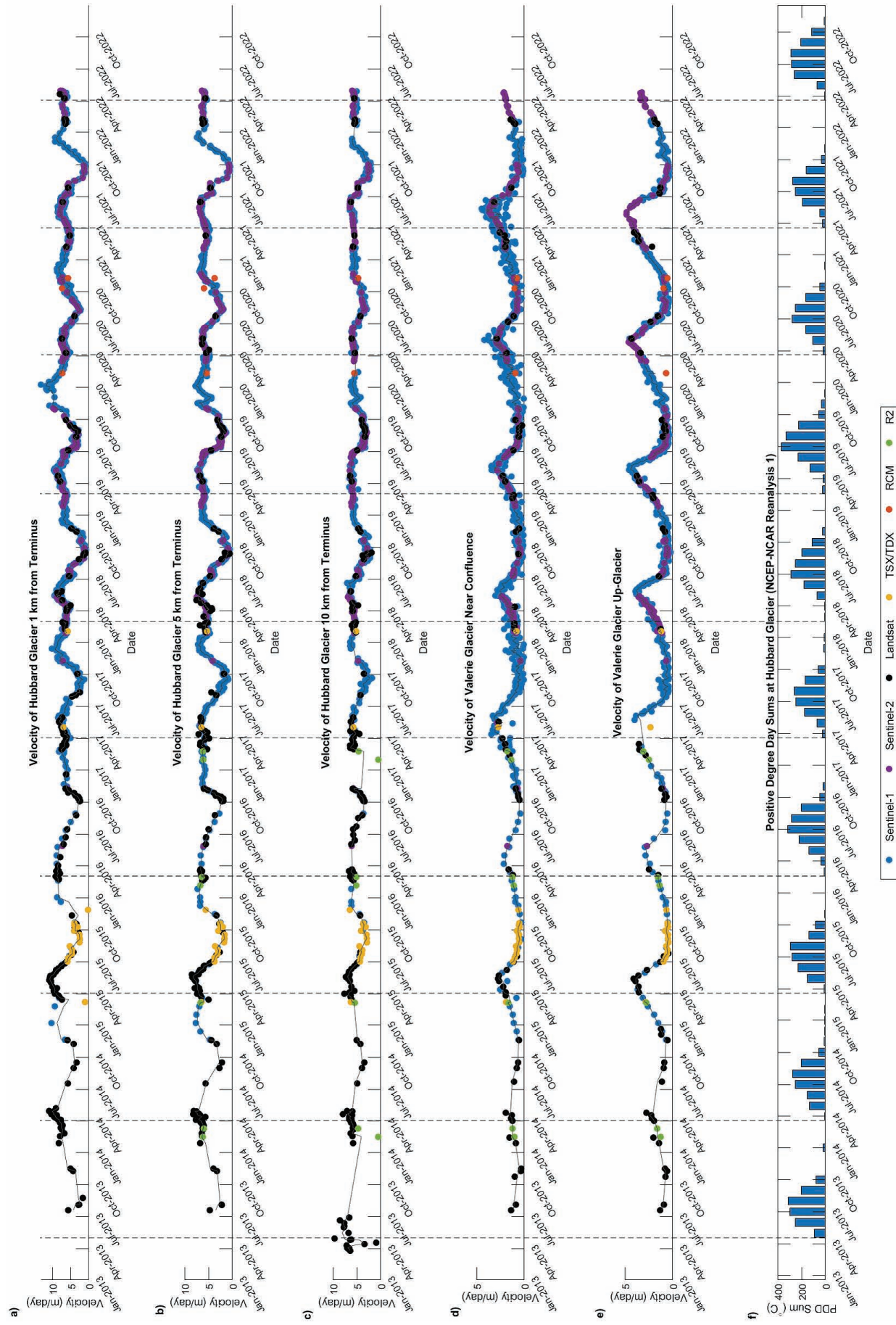


FIG 3. Velocity of Hubbard Glacier at 1 km (a), 5 km (b), and 10 km (c) from its terminus. The velocity of Valerie Glacier is shown near the confluence point with Hubbard Glacier (d) and further up-glacier (e). To graph the velocity data as a timeseries, a running mean line using $k = 3$ was used. The positive degree day (PDD) sums (f) are shown. Point locations are found in Figure 1. TSX/TDX is TerraSAR-X/TanDEM-X, RCM is RADARSAT Constellation Mission, and R2 is RADARSAT-2. Grey dashed lines represent the first spring month with $>5^{\circ}\text{C}$ PDD sum following the minimum winter/spring PDD sum value. RADARSAT Constellation Mission Imagery © Government of Canada (2020). RADARSAT is an official mark of the Canadian Space Agency.

DISCUSSION

Seasonality of Hubbard Glacier

Figure 4 displays a general conceptual presentation of Hubbard Glacier's seasonal patterns for our study period, including its inferred subglacial hydrology, ice motion, and melt.

The late spring/early summer velocity speedup on Hubbard Glacier follows the expected velocity response of a glacier to inputs of melt water into an inefficient subglacial drainage network (Willis, 1995; Nienow et al., 1998). For example, each year Hubbard Glacier's velocities increased until a velocity peak was observed in May (Figs. 3a-c, 4), which coincides with the increasing monthly PDD sums throughout the spring and summer (Fig. 3f). The velocity peak coinciding with melt suggests that early in the melt season (April and May each year; Fig. 3f), when PDD sums were increasing from month to month, the generated melt was drained to the glacier bed and into an inefficient subglacial drainage network. Input of melt to the bed led to increased glacier velocities (Figs. 3a–c, 4), as the glacier can slide more easily over a well lubricated bed (hard-bedded) or the water can propel more bed deformation (soft-bedded) (Willis, 1995).

The velocities of Hubbard Glacier decelerated each year after the May peak and reached the lowest velocities of the year in late summer/fall (Fig. 3a–c) over a period of time when monthly PDD sums were diminishing from their July–August peak until December (Fig. 3f). This evolution in dynamic response to air temperatures and, by proxy, surface melt, is likely explained by a switch to an efficient subglacial drainage system that is able to quickly transport surface meltwater through the englacial and subglacial drainage networks (Fig. 4). The efficient subglacial drainage system leads to less lubrication between the glacier and its bed, thereby increasing friction or decreasing till deformation, and causing flow speeds to decrease (Willis, 1995). This hypothesis is supported by the findings of Ritchie et al. (2008), who examined imagery and found that 50% of summers had embayments located on the terminus at Disenchantment Bay. These were likely caused by increased calving at the terminus front as a result of increased subglacial drainage, such that, from the summer to the fall, the embayment openings were visible, but were closed during the winter (Ritchie et al., 2008).

Each year, the flow speeds of Hubbard Glacier rebounded relatively quickly towards the winter peak after the annual velocity minimum observed in late summer/fall (Fig. 3a–c). To account for this behaviour, we argue that the overall fast movement of Hubbard Glacier may quickly cause ice deformation and destruction of the efficient subglacial channels that were developed during the summer, causing the distributed sub-glacier system to rapidly reform again (Nienow et al., 1998). The only way for efficient channels to enlarge or be maintained is if the amount of surface meltwater reaches the bed in appreciable quantities (Willis,

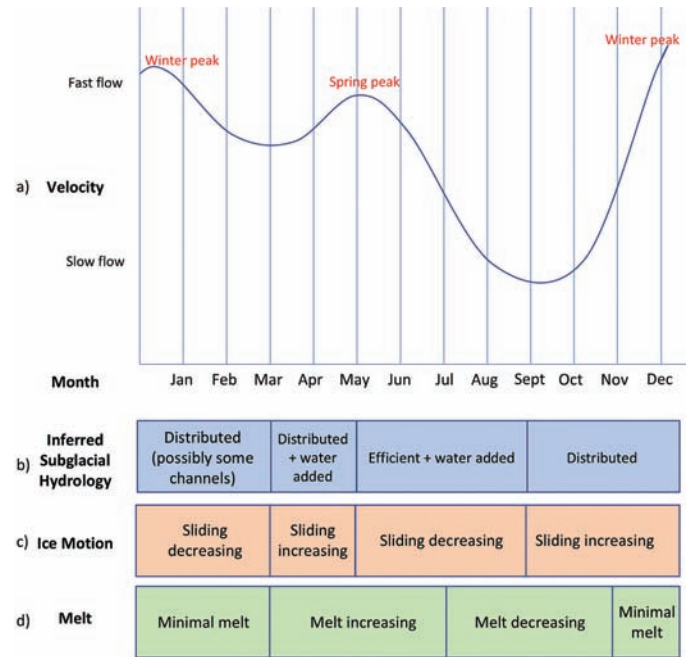


FIG 4. Hubbard Glacier's hypothesized seasonal patterns. The velocity plot shows the fast winter and spring peaks and minimums after each peak (a). Inferred subglacial hydrology is described as distributed or efficient (b). Ice motion describes whether sliding of the glacier on its bed is increasing or decreasing (c). Melt describes how much melt was observed from the PDD sums (d).

1995). Although PDD sums were greater than zero over this period, albeit diminishing from month to month after July–August each year (Fig. 3f), it is unlikely that the amount of melt generated was sufficient to maintain this efficient subglacial drainage network.

An interesting aspect of findings related to the Hubbard Glacier is the relatively high flow speeds that were reached during the winter season (between December and February annually; Figs. 3a–c, 4). It is difficult to determine the exact cause of the high winter velocities using a purely remote sensing-based approach, but we would like to consider a few possible theories. The cause of the winter speedup may be due to trapped water existing at high pressures in the subglacial channels, which can decrease friction at the bed (hard-bed) or facilitate bed deformation (soft-bed) and allow sliding to occur throughout the winter (Willis, 1995). It is also possible that increasing glacier thickness due to snow accumulation can increase deformation or basal motion, as was observed on Hintereisferner in Austria, which had slower summer velocities than annual speeds, even with little to no meltwater reaching the bed (Blümke and Finsterwalder, 1905, as cited in Willis, 1995). Another possibility is that liquid precipitation in the fall is reaching the bed of the glacier and increasing winter flow speeds (Yang et al., 2022). However, there are other possible mechanisms that can cause velocity changes (for example, ocean–ice interaction at the calving front, draining of supraglacial lakes, etc.) and these cannot be dismissed until further exploration of Hubbard Glacier's velocity pattern determines the cause.

High winter velocities of Hubbard Glacier were consistent in all years in this study, but this pattern was not found on Valerie Glacier (Fig. 3d–e), meaning that the process causing high flow rates for Hubbard Glacier at this time is likely influenced by the geometry of Hubbard Glacier. If the process was being driven solely by climate conditions, a similar winter velocity peak for Valerie Glacier would also be expected. The geometry of Hubbard and Valerie glaciers causing differences in seasonal flow speeds is supported by the hypothesis of Enderlin et al. (2018) stating that seasonal variations in flow speeds and basal drag are controlled through a glacier's geometry, which has a connection to its subglacial hydrology. Although Enderlin et al.'s (2018) study was focused on the geometry of retreating tidewater glaciers, evidence from the present study suggests that it is possible that this also applies to advancing tidewater glaciers.

After the velocity peak between December and February on Hubbard Glacier, velocities dropped slightly to reach a low point between February and April. Similar to the winter velocity peak, remote sensing did not allow us to determine the cause of the velocity decrease. However, it is possible that the subglacial hydrologic network may experience a minor reorganization, where water finds preferential paths to create some channels, leading to the drop in velocity. Alternatively, if precipitation events are the cause of the winter velocity increase (as put forth by Yang et al. [2022]), then this decrease in flow occurs because, in the late winter–early spring, water from rainfall no longer reaches the bed.

It is important to note that seasonal variations on Hubbard Glacier are most pronounced 1 km from the terminus, meaning this process may be linked to ocean processes at the calving front. It is also possible that the increased velocity variability further down-glacier may be caused by pressure variations from variations in surface water input (Willis, 1995). These pressure variations can be the result of higher melt rates in the lower ablation area, having thinner snowpacks further down-glacier (this decreases the attenuating influence), and an increased chance of the creation of an efficient englacial hydrologic system down-glacier (Willis, 1995). However, Willis (1995) attributed this efficient system to lower ice-deformation rates in the down-glacier region, which was not observed on Hubbard Glacier. Water pressure down-glacier more probably makes up a higher percentage of the ice overburden pressure compared to regions further up-glacier (Willis, 1995).

Hubbard Glacier's Seasonal Flow in Context

The large amount of velocity data provided in this study represents a significant improvement to the understanding of the seasonality of flow of Hubbard Glacier compared to previous studies. Studies by Stearns et al. (2015) and Trabant et al. (2003) both found highest flows in spring and slowest flows in fall. However, neither of those works

described the fast overall motion during the winter months reported here. Differences in the seasonal pattern may arise from our use of data with a higher temporal resolution. Conversely, Stearns et al. (2015) determined winter velocities by averaging fall to spring data, which could have averaged out the winter velocity peak. Trabant et al. (2003), meanwhile, analyzed two different velocity datasets: one from a fixed location, consisting of 22 image pairs, the other from a moving location with 11 velocity measurements. The limited amount of speed measurements in the latter study might have resulted in the research failing to capture this pattern. The amount of data used in our study was not available until SAR became popular and an increased number of sensors were launched, allowing our research to characterize seasonality on Hubbard and Valerie glaciers in a way that was not possible in the past.

Moon et al. (2014) provided one of the largest characterizations of seasonal patterns of ice motion using records of tidewater glacier motion, albeit from Greenland. These characterizations were further supported by Solgaard et al. (2022). However, Hubbard Glacier's seasonal flow (Fig. 4) does not fit exactly into any of the categories identified by Moon et al. (2014), which further demonstrates the uniqueness of this behaviour. This difference might arise from the number of observations used, as only three to six measurements were performed annually from 2009–13 for the glaciers Moon et al. (2014) studied, although more frequent measurements were done for a few glaciers. Kehrl et al. (2017) found that Kangerlussuaq Glacier in Greenland behaved similarly to what we present here for Hubbard Glacier, with a velocity peak in summer due to temperatures increasing meltwater that reaching the bed, and a velocity peak in the winter due to the iceshelf retreat.

Columbia and Post glaciers are tidewater glaciers located in Alaska that also experience interannual velocity changes in a similar way to Hubbard Glacier. Enderlin et al. (2018) attributed the seasonal velocity patterns seen in these glaciers to changes to the subglacial hydrological network, and both glaciers had larger variations in flow speeds closer to their termini than further up-glacier (Enderlin et al., 2018). Enderlin et al. (2018) used 89 velocity fields from 2012–16, and despite the similarities of Columbia Glacier and Hubbard Glacier, the first half of their study period showed Columbia and Post glaciers generally reached maximum velocities in May–June, then saw a rapid drop to reach minimum velocities in October–November (Enderlin et al., 2018). However, in 2014, Post Glacier showed unusual flow behaviour, with increased flow speeds and two velocity peaks, which is similar to the pattern we observed on Hubbard Glacier (Enderlin et al., 2018). Still, the behaviour of Post Glacier differed from that of Hubbard Glacier, as, that anomalous year on the former, flow speeds were much higher than average before dropping much lower than average for the 2015 minimum, a change that was not observed on Hubbard Glacier, where the pattern of two velocity peaks occurred in all years analyzed, from January 2017 to January 2022. (Enderlin et al., 2018). Although

there are differences between the results of Enderlin et al. (2018) and what is reported here, it would be interesting for future work to study Columbia and Post glaciers at the same resolution of Hubbard and Valerie glaciers to determine if Hubbard Glacier's unique seasonal pattern is also observed on similar glaciers (i.e., large size, tidewater) when the density of data allows the observation. Hubbard Glacier's seasonal behaviour would have previously been considered unusual for Alaska, although it is likely that previous studies never observed this seasonal pattern due to their sparse data density compared to that which is presented here.

Yang et al. (2022) found that within the Kenai Peninsula in Alaska, glaciers flowed in a similar way to that observed at Hubbard Glacier, with a velocity peak in May, decreasing velocities until a September–October minimum, and increasing velocities until a secondary peak in November. This velocity pattern was observed across many glaciers and different glacier types (land-terminating, tidewater-terminating, lake-terminating), although with varying amplitudes (Yang et al., 2022). Much like we have hypothesized regarding our finding, Yang et al. (2022) point to changing subglacial drainage systems from meltwater as the cause of the spring speedup and following slowdown. However, they attribute the cause of increased glacier motion in the early winter across the entire peninsula to regional-scale high precipitation rates that occur in the fall. We did not analyze precipitation for Hubbard and Valerie glaciers, although, it is possible that regional-scale precipitation is the cause of the winter speedup on Hubbard Glacier. Analyzing the effect of precipitation on these glaciers should be the focus of future work, as Valerie Glacier, though neighbouring and connected to it, does not show the same pattern of winter ice motion as Hubbard Glacier (possibly due to differences in glacier geometry, as discussed in the previous section); this contrasts with the synchronous short-term speed patterns of glaciers across the Kenai Peninsula (Yang et al., 2022). However, this pattern of seasonal glacier behaviour may be more common in Alaska than previous studies have shown, as a temporally dense velocity dataset throughout the entire year was needed to display this on Hubbard Glacier, and with similar findings now shown on Post Glacier (Enderlin et al., 2018) and in the Kenai Peninsula (Yang et al., 2022).

Seasonality of Valerie Glacier

Figure 5 summarizes Valerie Glacier's seasonal behaviour, showing the seasonal changes to its velocity, inferred subglacial hydrology, ice motion, and melt. Valerie Glacier showed a very traditional melt-induced flow variability signal that can be explained in the same way as the spring peak on Hubbard Glacier: through changes to subglacial hydrology (Willis, 1995). Velocities of Valerie Glacier increased until reaching the spring peak, coincident with warming temperatures that increased melt. Based on our inference and considering findings by Willis (1995),

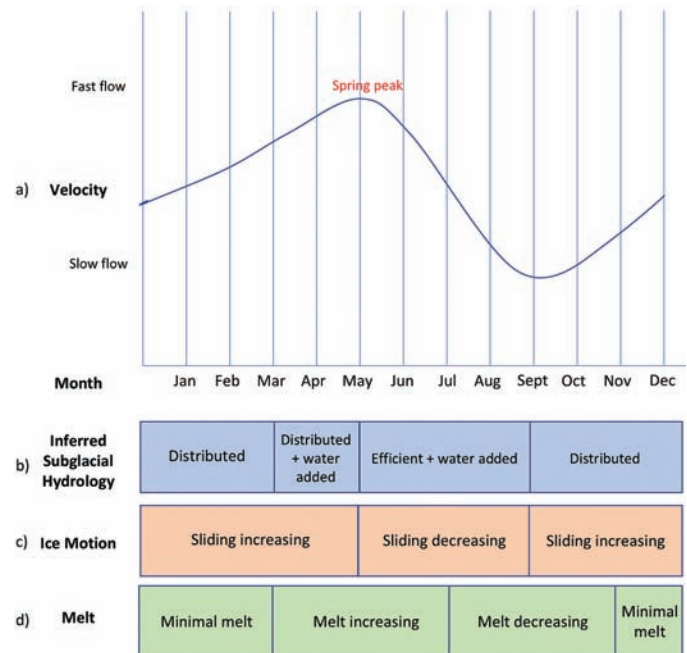


FIG 5. Valerie Glacier's hypothesized seasonal patterns. The velocity plot shows maximum velocity in the spring, followed by minimum velocities in the fall (a). Inferred subglacial hydrology describes whether the system is distributed or efficient (b). Ice motion describes whether the glacier's sliding on its bed is increasing or decreasing (c). Melt describes how much melt was observed from the PDD sums (d).

melt was then delivered to the glacier bed and increased basal water pressure. During this time, the discharge of water out from beneath the glacier is likely low to moderate, leading to lubrication of the glacier bed and a short-term increase in flow speeds (Willis, 1995). As the melt season progresses, the distributed network that leads to the spring velocity peak evolves, becoming a channelized, or efficient system by the end of the melt season, leading to termination of fast spring velocities. This is followed by intermediate summer velocities and minimum velocities in later summer/fall (Nienow et al., 1998; Armstrong et al., 2017). The melt driving velocity change is supported by the distribution of PDD sums (Fig. 3), with peak melt conditions occurring with velocity minimums. Valerie Glacier experienced gradually increasing velocities following the minimum fall velocities, suggesting that the efficient channels evolve back to a distributed system because of ice deformation (Nienow et al., 1998).

This behaviour differed from Hubbard Glacier. Valerie Glacier experienced only one velocity peak and one velocity drop each year, while Hubbard Glacier had two velocity peaks and drops. The winter velocity peak observed on Hubbard Glacier did not exist on Valerie Glacier, although they both had a spring peak around the same time each year, and late summer/fall minimums. Valerie Glacier's fastest velocities were in the spring, as opposed to Hubbard Glacier's fastest velocities, which were commonly observed in the winter. Also, after reaching its minimum velocities, Valerie Glacier did not rebound to faster velocities as quickly as Hubbard Glacier did, and in comparison, the

former had a more gradual speedup until its spring peak was reached again. The slower acceleration of Valerie Glacier may have been caused by its slower velocities than Hubbard Glacier, which would have taken longer to destroy the efficient drainage network.

CONCLUSIONS

This study examined the seasonality of Hubbard and Valerie glaciers at a higher temporal resolution than previously possible and provided the densest velocity record of Hubbard and Valerie glaciers ever created. This record reveals that the seasonal variability of ice flow on Hubbard Glacier increases when moving towards its calving front. This glacier experiences two velocity peaks and drops throughout the year: one in the spring (May) before dropping to minimum velocities in late summer/fall (August–October), and another peak in the winter (December–February), before dropping slightly between February and April. Hubbard Glacier's behaviour is different from that of Valerie Glacier, which experiences one velocity peak in the spring (May) before dropping to minimum flow speeds between August and November. We argue (following Willis, 1995) that the summertime velocity peak of both glaciers is caused by rising air temperatures increasing meltwater and raising water pressure at the bed, which allows enhanced basal sliding (Willis, 1995). Once seasonal melt increases enough, efficient channels form, leading to minimum velocities in late summer/fall, generally around when PDD values are decreasing, but still high (Nienow et al., 1998; Armstrong et al., 2017). We surmise (following Nienow et al., 1998) that the efficient drainage channels on both glaciers shift back to a distributed system due to ice deformation, leading the glaciers to speed up, although Hubbard Glacier does so at a faster rate than Valerie Glacier, likely due to its faster velocities (Nienow et al., 1998). Although there are similarities between Hubbard and Valerie glaciers and Columbia and Post glaciers, there are differences between their seasonality (Enderlin et al., 2018). However, we see similar seasonal velocity patterns now being observed in the Kenai Peninsula (Yang et al., 2022). Work by Enderlin et al. (2018) and Yang et al. (2022), as well as this study, show that the double peak velocity pattern may be more common in Alaska than previously thought.

While we did not determine the cause of the wintertime velocity peak we observed on Hubbard Glacier, we

hypothesized a few mechanisms for fast velocities. First, this may be due to water trapped beneath the glacier, although the mechanism of increased velocities differs depending on whether Hubbard Glacier has a hard or soft bed (Willis, 1995). If a hard bed exists, fast winter velocities may result from water increasing lubrication beneath the bed, whereas, if it has a soft bed, it might have fast winter velocities from water causing bed deformation or till failure (Willis, 1995). Second, fast winter velocities may be caused by increased ice deformation or basal motion by increased basal deformation and regelation due to increasing thickness from snow accumulation (Blümcke and Finsterwalder, 1905, as cited in Willis, 1995). Lastly, it is possible that rainwater in the fall increased winter flow speeds (Yang et al., 2022). Since we did not find fast winter velocities on neighbouring Valerie Glacier, it is likely that the driver of the winter velocity peak is affected by Hubbard Glacier's the geometry. This study cannot draw any firm conclusions about the cause of the velocity drop after the winter velocity peak, although we hypothesized that water may be finding preferential paths and increasing the efficiency of the subglacial drainage before being destroyed by the fast velocities and becoming fully distributed again to reach the spring peak, or due to decreased rainwater input reaching the bed. Future work could focus on causes of the winter velocity peak and subsequent velocity drop, as it is possible that other causes besides the hydrologic network are influencing Hubbard Glacier's seasonal velocity trend (for example, ocean-ice interaction at the calving front, or supraglacial lake drainage). Other glaciers could be behaving similarly, although their velocity data was not temporally dense enough to see this pattern.

ACKNOWLEDGEMENTS

We acknowledge the support of the Natural Sciences and Engineering Research Council of Canada (NSERC), [CGS-M to CB and Discovery Grant (RGPIN-02443-2021) to WvW. Cette recherche a été financée par le Conseil de recherches en sciences naturelles et en génie du Canada (CRSNG), (CGS-M à CB et de subventions à la découverte [RGPIN-02443-2021] à WvW). We also acknowledge the support of the Canada Foundation for Innovation (John R. Evans Leadership Fund), the Ontario Research Fund, Environment and Climate Change Canada – Climate Research Division, the University of Waterloo, and ArcticNet Network of Centres of Excellence Canada. TerraSAR-X data are available through the DLR (©DLR 2023).

REFERENCES

- Airbus Defence and Space. 2014. TerraSAR-X image product guide: Basic and enhanced radar satellite imagery. https://www.engesat.com.br/wp-content/uploads/r459_9_201408_tsxx-itd-ma-0009_tsx-productguide_i2.00.pdf
- Armstrong, W.H., Anderson, R.S., and Fahnestock, M.A. 2017. Spatial patterns of summer speedup on south central Alaska glaciers. *Geophysical Research Letters* 44(18):9379–9388. <https://doi.org/10.1002/2017GL074370>

- Blümcke, A., and Finsterwalder, S. 1905. Zeitliche Änderungen in der Geschwindigkeit der Gletscherbewegung [Temporal change in the speed of glacier movement]. *Sitzungsberichte der mathematisch-physikalischen Klasse der Kgl. Bayerischen Akademie der Wissenschaften zu München* 35(1):109–131.
- Burgess, E., Forster, R., and Larsen, C. 2013a. Flow velocities of Alaskan glaciers. *Nature Communications* 4: 2146. <https://doi.org/10.1038/ncomms3146>
- Burgess, E.W., Larsen, C.F., and Forster, R.R. 2013b. Summer melt regulates winter glacier flow speeds throughout Alaska. *Geophysical Research Letters* 40(23):6160–6164. <https://doi.org/10.1002/2013GL058228>
- Clarke, G.K.C., and Holdsworth, G. 2002. Glaciers of North America—Glaciers of Canada: Glaciers of the St. Elias Mountains. In: Williams, R.S., and Ferrigno, J.G., eds. *Satellite image atlas of glaciers of the world*. U.S. Geological Survey Professional Paper 1386-J-1. <https://pubs.usgs.gov/pp/p1386j/stelias/stelias-lores.pdf>
- European Space Agency. 2020. About Copernicus sentinel-2. <https://sentinel.esa.int/documents/247904/4180891/Sentinel-2-infographic.pdf>
- . 2021. About Copernicus-1. <https://sentinels.copernicus.eu/documents/247904/4603794/Sentinel-1-infographic.pdf>
- Enderlin, E.M., O’Neal, S., Bartholomaus, T.C., and Joughin, I. 2018. Evolving environmental and geometric controls on Columbia Glacier’s continued retreat. *Journal of Geophysical Research: Earth Surface* 123(7):1528–1545, <https://doi.org/10.1029/2017JF004541>
- Gardner, A.S., Moholdt, G., Scambos, T., Fahnestock, M., Ligtenberg, S., van den Broeke, M., and Nilsson, J. 2018. Increased west Antarctic and unchanged east Antarctic ice discharge over the last 7 years. *The Cryosphere* 12:521–547. <https://doi.org/10.5194/tc-12-521-2018>
- Gardner, A.S., Fahnestock, M.A., and Scambos, T.A. 2021. MEaSUREs ITS_LIVE landsat image-pair glacier and ice sheet surface velocities: Version 1 (Beta). http://its-live-data.jpl.nasa.gov.s3.amazonaws.com/documentation/ITS_LIVE-Landsat-Scene-Pair-Velocities-v01.pdf
- Gardner, A.S., Fahnestock, M.A., and Scambos, T.A. 2022. MEaSUREs ITS_LIVE landsat image-pair glacier and ice sheet surface velocities. (Data set ID: NSIDC-0775, Version 1). Boulder, Colorado USA. NASA National Snow and Ice Data Center Distributed Active Archive Center. Accessed 30 November 2022 and 14 December 2023. http://its-live-data.jpl.nasa.gov.s3.amazonaws.com/documentation/ITS_LIVE-Landsat-Scene-Pair-Velocities-v01.pdf
- Government of Canada. 2021. January 12. RADARSAT satellites: Technical comparison. <https://www.asc-csa.gc.ca/eng/satellites/radarsat/technical-features/radarsat-comparison.asp>
- Kehrl, L.M., Joughin, I., Shean, D.E., Floricioiu, D., and Krieger, L. 2017. Seasonal and interannual variabilities in terminus position, glacier velocity, and surface elevation at Helheim and Kangerlussuaq Glaciers from 2009 to 2016. *Journal of Geophysical Research: Earth Surface* 122(9):1635–1652. <https://doi.org/10.1002/2016JF004133>
- Main, B., Copland, L., Smeda, B., Kochtitzky, W., Samsonov, S., Dudley, J., Skidmore, M., et al. 2022. Terminus changes of Kaskawulsh Glacier, Yukon, under a warming climate: Retreat, thinning, slowdown and modified proglacial lake geometry. *Journal of Glaciology* 69(276): 936–952. <https://doi.org/10.1017/jog.2022.114>
- Mayo, L.R. 1988. Advance of Hubbard Glacier and closure of Russell Fiord, Alaska—Environmental effects and hazards in the Yakutat area. In: Galloway, J.P., and Hamilton, T.D., eds. *Geologic studies in Alaska by the U.S. Geological Survey during 1987*. U.S. Geological Survey Circular 1016:4–16.
- Mayo, L. 1989. Advance of Hubbard Glacier and 1986 outburst of Russell Fiord, Alaska, U.S.A. *Annals of Glaciology* 13:189–194. <https://doi.org/10.3189/S0260305500007874>
- Meier, M.F., and Post, A. 1987. Fast tidewater glaciers. *Journal of Geophysical Research* 92(B9):9051–9058. <https://doi.org/10.1029/JB092iB09p09051>
- Moon, T., Joughin, I., Smith, B., van den Broeke, M.R., van der Berg, W.J., Noël, B., and Usher, M. 2014. Distinct patterns of seasonal Greenland glacier velocity. *Geophysical Research Letters* 41(20):7209–7216. <https://doi.org/10.1002/2014GL061836>
- Nienow, P., Sharp, M., and Willis, I. 1998. Seasonal changes in the morphology of the subglacial drainage system, Haut Glacier D’Arolla, Switzerland. *Earth Surface Processes and Landforms* 23(9):825–843. [https://doi.org/10.1002/\(SICI\)1096-9837\(199809\)23:9<825::AID-ESP893>3.0.CO;2-2](https://doi.org/10.1002/(SICI)1096-9837(199809)23:9<825::AID-ESP893>3.0.CO;2-2)
- NOAA (National Oceanic and Atmospheric Administration). 2025. NCEP–NCAR reanalysis 1. <https://psl.noaa.gov/data/gridded/data.ncep.reanalysis.html>
- RGI Consortium 2017. Randolph Glacier inventory—A dataset of global glacier outlines. Data set NSIDC-0770, Version 6. National Snow and Ice Data Center. Accessed 15 September 2022. <https://doi.org/10.7265/4mlf-gd79>

- Ritchie, J., Lingle, C., Motyka, R., and Truffer, M. 2008. Seasonal fluctuations in the advance of a tidewater glacier and potential causes: Hubbard Glacier, Alaska, USA. *Journal of Glaciology* 54(186):401–411.
<https://doi.org/10.3189/002214308785836977>
- Samo, L. 2022. Investigation of intra-annual velocity and seasonality of White and Thompson Glaciers, Axel Heiberg Island, Nunavut. Master's Thesis, University of Waterloo, Waterloo, Ontario.
<https://dspacemainprd01.lib.uwaterloo.ca/server/api/core/bitstreams/662a40c5-4528-4ale-aedb-2ec4108825cd/content>
- Solgaard, A.M., Rapp, D., Noël, B.P.Y., and Hvidberg, C.S. 2022. Seasonal patterns of Greenland ice velocity from Sentinel-1 SAR data linked to runoff. *Geophysical Research Letters* 49(24): e2022GL100343..
<https://doi.org/10.1029/2022GL100343>
- Stearns, L.A., Hamilton, G.S., van der Veen, C.J., Finnegan, D.C., O'Neil, S., Scheick, J.B., and Lawson, D.E. 2015. Glaciological and marine controls on terminus dynamics of Hubbard Glacier, southeast Alaska. *Journal of Geophysical Research: Earth Surface* 120(6):1065–1081.
<https://doi.org/10.1002/2014JF003341>
- Strozzi, T., Luckman, A., Murray, T., Wegmüller, U., and Werner, C.L. 2002. Glacier motion estimation using SAR offset-tracking procedures. *IEEE Transactions on Geoscience and Remote Sensing* 40(11):2384–2391.
<https://doi.org/10.1109/TGRS.2002.805079>
- Trabant, D.C., Krimmel, R.M., and Post, A. 1991. A preliminary forecast of the advance of Hubbard Glacier and its influence on Russell Fiord, Alaska. *Water-Resources Investigations Report 90-4172*. U.S. Geological Survey.
<https://doi.org/10.3133/wri904172>
- Trabant, D., Krimmel, R.M., Echelmeyer, K.A., Zirnheld, S.L., and Elsberg, D.H. 2003. The slow advance of a calving glacier: Hubbard Glacier, Alaska, U.S.A. *Annals of Glaciology* 36:45–50.
<https://doi.org/10.3189/172756403781816400>
- U.S. Geological Survey. 2022. Landsat 9 data users handbook. Version 1.0.
https://d9-wret.s3.us-west-2.amazonaws.com/assets/palladium/production/s3fs-public/media/files/LSDS-2082_L9-Data-Users-Handbook_v1.pdf
- Van Wychen, W., Copland, L., Gray, L., Burgess, D., Danielson, B., and Sharp, M. 2012. Spatial and temporal variation of ice motion and ice flux from Devon Ice Cap, Nunavut, Canada. *Journal of Glaciology* 58(210):657–664.
<https://doi.org/10.3189/2012JoGl11J164>
- Van Wychen, W., Davis, J., Burgess, D.O., Copland, L., Gray, L., Sharp, M., and Mortimer, C. 2016. Characterizing interannual variability of glacier dynamics and dynamic discharge (1999–2015) for the ice masses of Ellesmere and Axel Heiberg Islands, Nunavut, Canada. *Journal of Geophysical Research Earth Surface* 121(1):39–63.
<https://doi.org/10.1002/2015JF003708>
- Van Wychen, W., Copland, L., Jiskoot, H., Gray, L., Sharp, M., and Burgess, D. 2018. Surface velocities of glaciers in western Canada from speckle-tracking of ALOS PALSAR and RADARSAT-2 data. *Canadian Journal of Remote Sensing* 44(1):57–66.
<https://doi.org/10.1080/07038992.2018.1433529>
- Van Wychen, W., Bayer, C., Copland, L., Brummell, E., and Dow, C. 2023. Radarsat constellation mission derived winter glacier velocities for the St. Elias Icefield, Yukon/Alaska: 2022 and 2023. *Canadian Journal of Remote Sensing* 49(1): 22643995.
<https://doi.org/10.1080/07038992.2023.2264395>
- Waechter, A., Copland, L., and Herdes, E. 2015. Modern glacier velocities across the Icefield Ranges, St. Elias Mountains, and variability at selected glaciers from 1959 to 2012. *Journal of Glaciology* 61(228):624–634.
<https://doi.org/10.3189/2015JoGl14J147>
- Willis, I.C. 1995. Intra-annual variations in glacier motion: A review. *Progress in Physical Geography: Earth and Environment* 19(1): 61–106.
<https://doi.org/10.1177/030913339501900104>
- Yang, R., Hock, R., Kang, S., Guo, W., Shangguan, D., Jiang, X., and Zhang, Q. 2022. Glacier surface speed variations on the Kenai Peninsula, Alaska, 2014–2019. *JGR Earth Surface* 127(3): e2022JF006599.
<https://doi.org/10.1029/2022JF006599>